CURRENT DEVELOPMENTS AND FUTURE CHALLENGES IN PHYSICS ANALYSES OF THE NRU HEAVY WATER RESEARCH REACTOR

S. Nguyen, B. Wilkin and T. Leung
AECL Chalk River Laboratories, Chalk River
Ontario, CANADA KOJ 1J0
nguyens@aecl.ca, wilkinb@aecl.ca, leungt@aecl.ca

Abstract

The National Research Universal (NRU) reactor is heavy water cooled and moderated, with on-power fueling capability. TRIAD, a 3D two-group diffusion code, is currently used for support of day-to-day NRU operations. Recently, an MCNP full reactor model of NRU has been developed for benchmarking TRIAD. While reactivity changes and flux and power distributions from both methods are in reasonably good agreement, MCNP appears to eliminate a *k*-eff bias in TRIAD. Beyond TRIAD's capability, MCNP enables the assessment of radiation in the NRU outer structure. Challenges include improving TRIAD accuracy and MCNP performance, as well as performing NRU core-following using MCNP.

1. Introduction

The National Research Universal (NRU) reactor at Chalk River Laboratories began operation in 1957. It is used to carry out research in basic science and in support of the CANDU power reactor programs, such as fuel bundle and material development, and is also a major supplier of medical radioisotopes world-wide. The NRU reactor is heavy water cooled and moderated, with on-power refueling capability. It is licensed to operate at a maximum power of 135 MW, and has a peak thermal neutron flux of about 4.0E+14 n.cm^{-2}.s^{-1}.

Figure 1 shows an NRU core lattice, with 31 rows (numbered) and 18 columns (lettered). The hexagonal lattice pitch is 19.685 cm. The NRU core consists of many different types of rods, such as driver fuel rods, fast-neutron rods, Mo-99 production rods, test loops, and various absorber rods. There are 227 rod sites in the NRU core, including 18 control rods and 4 adjuster rods.

This paper describes current developments and future challenges in the physics analysis of the NRU reactor, using both the TRIAD deterministic code and the MCNP stochastic (Monte Carlo) code.

2. TRIAD method

The TRIAD code [1], a 3D, two-group diffusion code, has been used to perform various physics calculations in support of day-to-day NRU operations, including power distribution for determining depletion in core assemblies, reactivity calculations for determining rod worths for on-power refueling, control rod worths, the reactivity worth of voiding the coolant in a loop, and neutron flux distributions throughout the core.

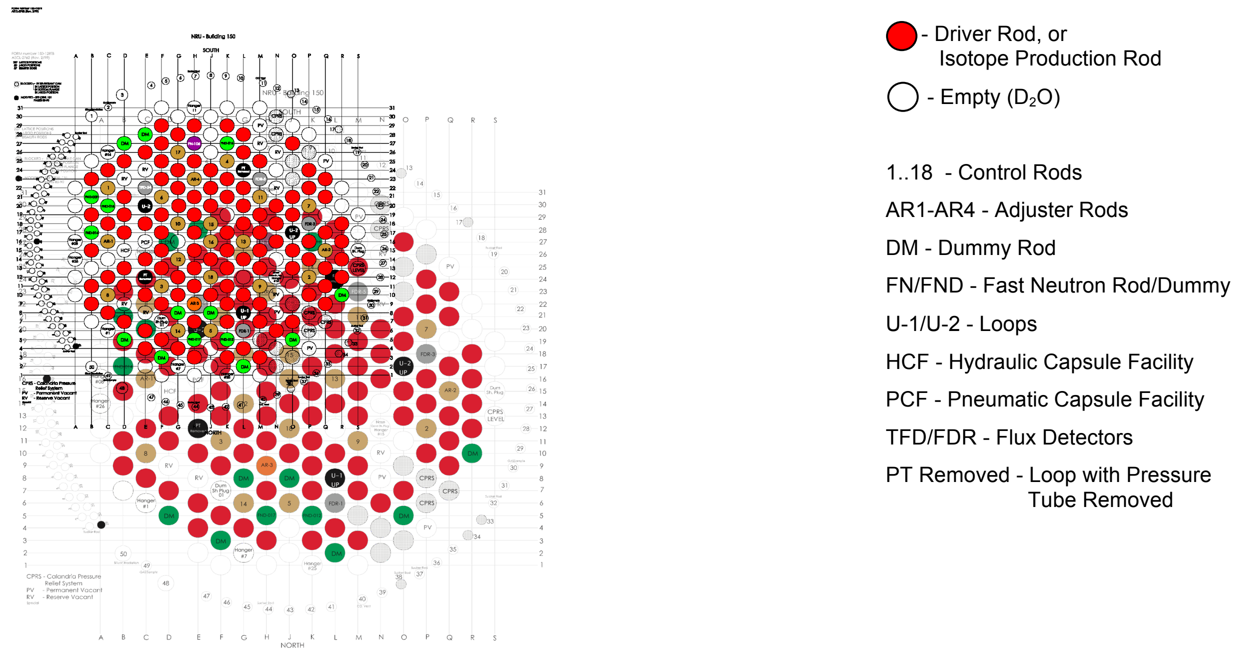

Figure 1 The modeled NRU core lattice

The TRIAD code has two main modules. The first is the simulation module which calculates steady-state neutron flux and power distributions in the reactor. The present TRIAD version incorporates 301 hexagonal sites, each comprising six triangular prisms, with 18 axial segments of variable heights. There is a total of $6\times301\times18$ triangular prisms (or meshes) for the whole reactor. The 18 axial cells representing a rod in NRU can be of different cell types, each with uniform neutronic properties. The detailed flux shapes and neutron spectra through each type of cell are determined using the WIMS-AECL neutron transport code [2]. The homogenized cell parameters, in two energy groups, are then calculated by flux- and volume-weighting the region material properties. Examples of cell parameters are the diffusion coefficients and the various cross sections, such as absorption, removal and fission.

After the cell parameters are calculated, the flux and power distributions for the cells in the NRU core can be determined using a modified neutron diffusion theory. The modification is the use of cell discontinuity factors (*cdf*) to improve the radial neutron leakage calculation between adjacent cells. The usual inter-cell leakage calculation in finite-difference diffusion theory uses a simple linear model, which distorts the flux distribution except in relatively uniform reactors. Since the NRU reactor comprises many different types of rods, some with very different neutronic properties, it is necessary to use *cdf*'s in TRIAD to adjust the neutron current calculation at the homogeneous cell boundaries to minimize these distortions. The *cdf* is calculated from the ratio of the heterogeneous to homogeneous cell boundary fluxes in WIMS-AECL.

In the TRIAD code, the two-group diffusion equations in three dimensions are solved numerically using a finite difference method. The difference equations for the group fluxes in each triangular prism of an NRU hexagonal cell are solved using flux iteration techniques, with successive point over-relaxation to accelerate convergence. After the fluxes in all prisms are determined, the flux in each hexagonal cell is calculated as the average of the fluxes of the six triangular prisms for that cell. The power generated from a hexagonal cell is then calculated as the product of the cell flux, cell volume and Q-value, which is the linear heat rating per unit flux per unit cell volume.

The second module of TRIAD is the core-following module which tracks reactor assemblies by name, reactor position and fuel burnup, or isotopic content for isotope production rods, as they move into and out of the reactor. Reactor snapshots are stored as core loadings. A core loading contains the necessary data for all axial segments of each type of rod in the reactor, such as the linear burnup (in MWd/cm) in each axial segment for fuel assemblies, and the isotopic concentration (in g/cm) and activity (in Ci/cm) for isotope production rods. Rod changes, such as refuelling, may take place between two reactor snapshots. In the TRIAD core-following module, the run period between two snapshots is further divided into smaller rod-change intervals, and the fuel depletion (burnup accumulation) for each interval is calculated using a fixed representative power distribution. Both measured and simulated channel power distributions are used, together with the simulated axial power distributions (since there are no axial power distribution measurements). The measured channel powers are obtained from on-line rod coolant flow and temperature rise measurements in the reactor. For each rod-change interval, the accumulated burnup for a rod in the reactor is calculated by distributing the total reactor burnup increment among the power generating rods in the core. For the axial burnup increases for a rod, it is calculated using the ratio of axial power to total rod power from simulation.

In addition to calculating the axial burnups of fuel rods, the TRIAD core-following module also tracks the Mo-99, Co-60 and C-14 concentrations and activities in each axial section of the isotope production rods or absorbers for the run period.

3. MCNP method

Currently, the statistical MCNP method [4] cannot compete with TRIAD for support of daily NRU operation, but can be used for benchmarking the TRIAD key parameters, and for assessing data of interest that are *beyond* the capabilities of TRIAD.

3.1 Model

The MCNP model of NRU (Figure 2) includes not only the core but also the outer structure, generally ending at surfaces exposed to the ambient air. Since NRU is fairly large in both geometry and quantity of materials, a very detailed model would be challenging due to longer execution times, and, for now, computer memory limitations. Thus simplification is necessary to get a workable model, but at the expense of losing fine component detail.

The MCNP core configuration is closely based on the TRIAD core model (for comparison of results) by matching site to site, but each MCNP core site is modeled in greater detail to be as realistic as possible. For example, each driver fuel rod site is modeled explicitly with individual fuel pins installed in a flow tube, all submerged in heavy water. The fuel meat in each pin is axially segmented, to accommodate different fuel burnups as in TRIAD, as are the fuel elements in a loop fuel string.

Typically, a working NRU core is loaded with about 80 driver rods of various burnups ranging from 0 (fresh) to ~360 MWd/rod (exit burnup). The current model, however, can only accommodate about half that number of driver rod burnups (due to memory limitations). This is probably the most serious modeling restriction encountered to date, preventing the use of MCNP for modeling any *actual* NRU cores.

Except for driver rod and loop fuels, only unirradiated material compositions are used in the model. This keeps the number of cells to a minimum. In principle, they may be sub-divided to accommodate varying materials due to burnup (like irradiated fuels), but only at the expense of further reducing the number of driver rod burnups. Generally, irradiated fuel compositions are calculated outside the MCNP environment using WIMS/TRIAD (for driver rods) or WIMS/BURFEL (for loop fuels). BURFEL [5] is a code and database system for calculating and keeping track of NRU loop fuel powers and burnups.

There are two driver fuel MCNP models: the *single-burnup* core and the *multi-burnup* core. In the single-burnup model all driver fuel rods have the same axial burnup distribution, with the compositions containing more than 200 fission products generated using WIMS and the ENDF/B-VII library. In order to increase the maximum number of compositions possible in the MCNP multi-burnup model, WIMS was run with the ENDF/B-VI library producing less than 100 fission products for each composition. MCNP used the ENDF/B-VII library for both models.

The criticality calculation (KCODE source option) is normally used in MCNP, with both neutron and photon modes turned on. As in TRIAD, the normalization is set to 100 MW of reactor fission power, requiring the total core fission tally to be used. Other flux and/or energy tallies are also needed depending on the case requirements (putting in so many tally entries would greatly increase the computation time). Typically, 50 million source histories are required for an acceptable accuracy of the k-eff value (with a standard deviation $1\sigma < 0.1$ mk) or other in-core parameters (1σ of a few percent), but 10 times that may be needed to produce meaningful data beyond the core. Typical execution times vary from three to seven days on a WINDOWS-based computer cluster, depending on the resources assigned to the case. In comparison, TRIAD needs only a few minutes to complete a case.

There are two in-house MCNP patches (i.e., modifications) that enhance NRU modeling. The first patch allows the user to change the MCNP hard-coded fission q-values (which include only the *prompt* energy release components) to the *recoverable* energy release components that are used in WIMS/TRIAD, so that the calculated fission powers in both methods are consistent. For energy deposition (heating or dose rate) calculations, the second patch can be used to add the delayed beta and photon energies from decay of fission products and/or significant activation products. While the additional delayed beta energy is deposited locally, the delayed gamma energy is carried by the additional photons and deposited elsewhere.

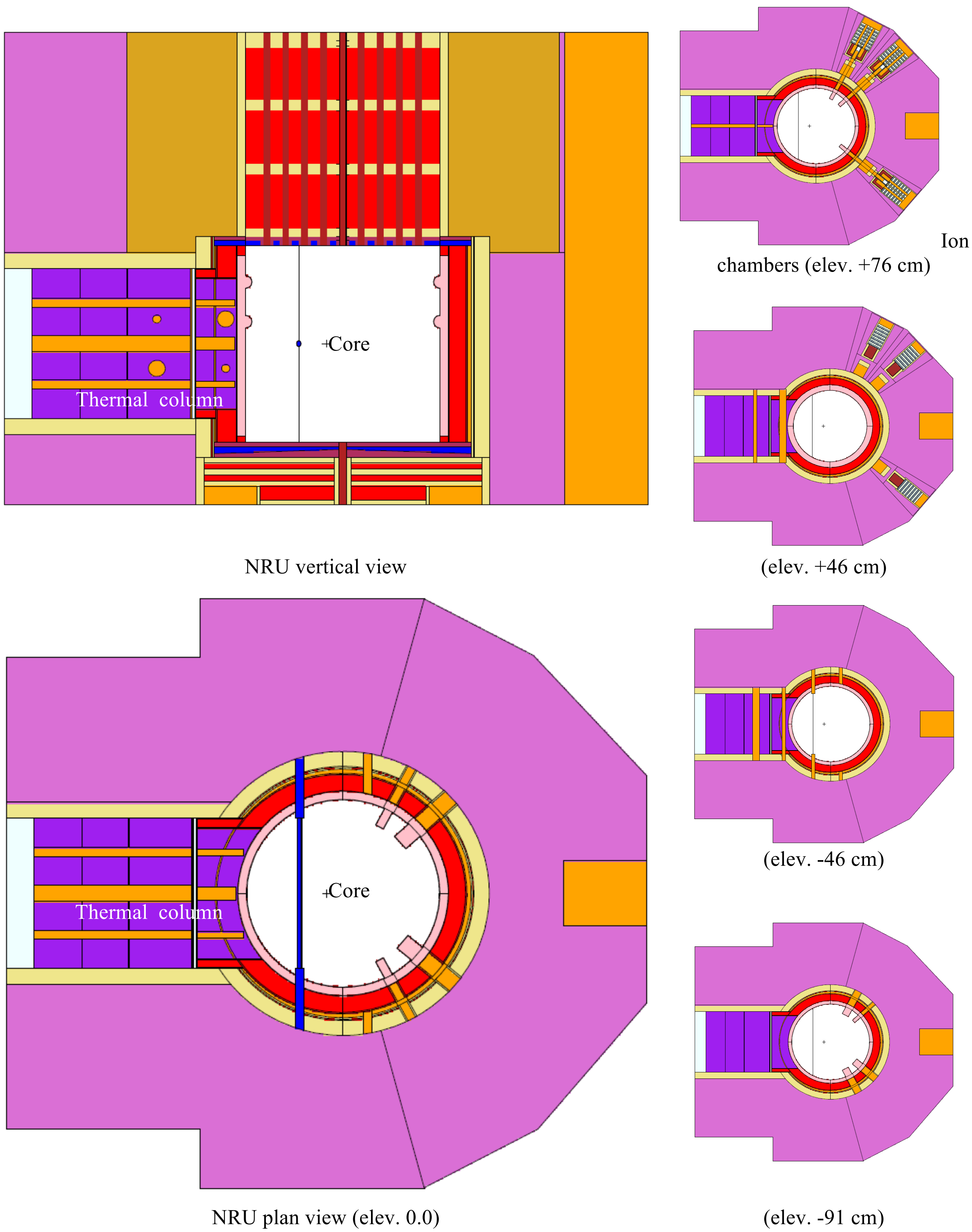

Figure 2 NRU outer structure – MCNP model

3.2 In-core parameter comparisons

Both MCNP and TRIAD calculations were performed on several simplified cores and their results were compared. The key parameters are *k*-eff, neutron flux and fission power distributions.

3.2.1 *k*-eff

Table 1 presents the *k*-eff and control rod worth values from MCNP and TRIAD for the *single-burnup* core model. This core configuration was similar to an NRU restart core in August 2010 but the driver fuel rods were all made identical, given the average rod burnup (note that the burnup still varied axially from segment to segment in each fuel pin). The NRU control rods listed in the table, which are also identical but located at different positions in the core, were raised in sequence. It is seen that while the control rod worth (Δk) was consistent for both methods, the MCNP *k*-eff was about 30 mk less than its TRIAD counterpart. Note here that TRIAD *k*-eff values have been validated to have a positive bias of about 30 mk [3], which appears to be eliminated by MCNP.

Table 1
Core *k*-eff and control rod worth

Control rod raised in sequence	TRIAD		MCNP		MCNP vs. TRIAD (Δk-eff, mk)
	k-eff	CR worth (Δk, mk)	*k*-eff (±0.01%)	CR worth (Δk, mk)	
CR#16 (base core*)	1.064788	14.8	1.03307	13.8	-31.7
CR#15	1.049982	12.0	1.01924	9.4	-30.7
CR#14	1.038023	2.5	1.00981	3.0	-28.2
CR#13	1.035538	14.1	1.00685	14.5	-28.7
CR#12	1.021470	3.5	0.99237	3.4	-29.1
CR#11	1.017969	-	0.98897	-	-29.0

* A single-burnup core with the first 16 control rods fully raised.

3.2.2 Fluxes and powers

Figure 3 and Figure 4 show the fission power and neutron flux distributions in driver rod J14 near the core centre in the respective single-burnup and multi-burnup cores (in the latter core, the driver rod burnup varied axially and from rod to rod).

In general, the axial power and flux distributions in a driver rod are consistent for both methods. There are discrepancies as expected since the two code models have significant differences, especially in the use of cell discontinuity factors (*cdf*) and diffusion theory boundary conditions in TRIAD. It can be seen that the more heterogeneous the driver rod burnup, the more deviation between the MCNP and TRIAD results, especially for the rod powers. Part of the reason for this is that TRIAD uses *cdf*'s, which are normally calculated in an azimuthally uniform environment and depend primarily on the burnup in the cell of interest. Also, the axial *cdf* in TRIAD is always equal to 1.0 despite the axially varying rod burnup.

MCNP gives more detailed power and flux distributions. The step changes in axial powers seen in Figure 4 are due to step changes in the modeled fuel burnup, but it would be too costly to use more segments to smooth the rod axial burnup distribution.

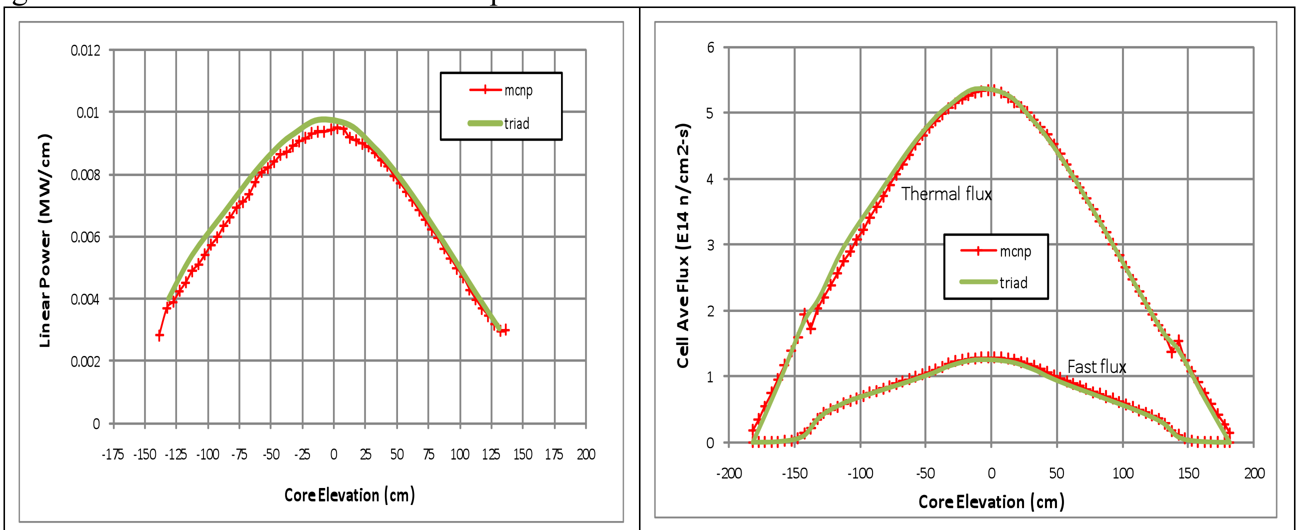

Rod Fission Power | Site Average Flux

Figure 3 Uniform driver rod J14 in a single-burnup core

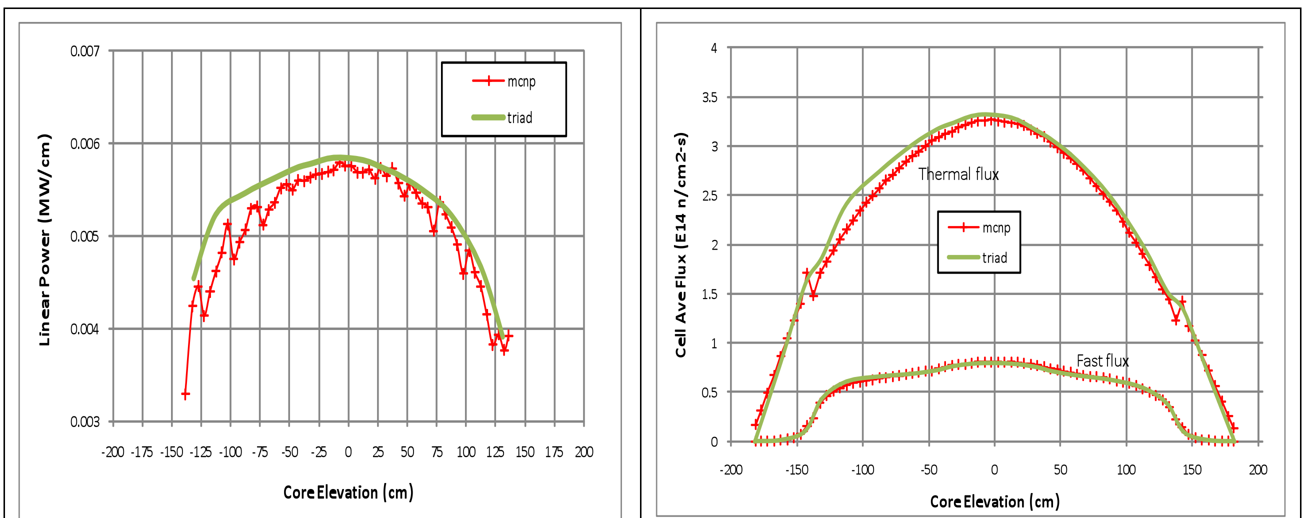

Rod Fission Power | Site Average Flux

Figure 4 Segmented driver rod J14 in a multi-burnup core

It can also be seen that the TRIAD axial distributions are slightly higher than MCNP in the lower half of the core. This is due to differences in the axial positioning of absorber rods in the two models.

Like TRIAD, MCNP can also provide the core power and flux maps. Figure 5 and Figure 6 compare the MCNP site fluxes and powers with the TRIAD counterparts in a *multi-burnup* core.

Compared to TRIAD, the MCNP radial thermal flux is slightly lower towards the core centre but higher towards the core periphery in the heavy water reflector sites. On the contrary, the MCNP above-thermal flux (>0.625 eV or TRIAD *fast* flux) in these reflector sites is significantly lower than the TRIAD counterpart. This indicates a possible deficiency in the TRIAD model near the core boundary, possibly due to edge effects. For the inner, most important sites, the flux (Figure 5) and power (Figure 6) from MCNP and TRIAD are consistent and similar (within 10%).

Thermal (<0.625 eV) Flux Ratios

34											---											34
33								---		---		---		---								33
32							---		1.03		1.00		0.98		---							32
31						---		1.02		1.00		0.98		0.95		---						31
30					---		0.98		0.99		0.98		0.96		0.78		---					30
29				---		0.96		0.98		0.98		0.96		0.92		0.90		---				29
28					0.97		0.96		0.97		0.97		0.95		0.88		0.92					28
27				1.01		0.95		0.96		0.96		0.96		0.95		0.93		0.78				27
26			---		0.97		0.94		0.96		0.98		0.96		0.97		0.83		---			26
25		---		1.00		0.94		0.95		0.96		0.97		0.97		0.98		0.92		---		25
24			1.02		0.97		0.93		0.95		0.96		0.96		1.00		0.98		1.03			24
23		---		0.99		0.94		0.93		0.94		0.95		1.00		1.01		1.02		---		23
22			1.03		0.96		0.95		0.94		0.95		0.98		1.02		1.03		1.06			22
21		1.12		0.98		0.96		0.93		0.93		0.95		1.00		1.03		1.05		1.10		21
20	---		1.01		0.96		0.95		0.92		0.94		0.97		1.02		1.05		1.08		---	20
19		1.06		0.96		0.93		0.92		0.91		0.95		0.98		1.03		1.07		1.11		19
18	---		0.99		0.93		0.90		0.90		0.93		0.95		1.00		1.06		1.10		---	18
17		1.05		0.95		0.90		0.87		0.91		0.94		0.98		1.04		1.08		1.11		17
16	---		0.99		0.93		0.89		0.89		0.92		0.95		0.99		1.05		1.08		---	16
15		1.03		0.95		0.91		0.88		0.89		0.94		0.95		1.01		1.05		1.11		15
14	---		0.98		0.93		0.89		0.88		0.93		0.95		0.97		1.02		1.08		---	14
13		1.02		0.95		0.91		0.87		0.90		0.94		0.95		1.00		1.05		1.09		13
12	---		0.98		0.93		0.88		0.87		0.92		0.95		0.99		1.01		1.04		---	12
11		1.04		0.95		0.90		0.88		0.90		0.96		0.98		0.99		1.01		1.06		11
10			0.97		0.92		0.89		0.87		0.92		0.98		0.99		0.97		0.99			10
9		---		0.95		0.90		0.89		0.92		0.97		0.98		0.97		0.94		---		9
8			0.95		0.94		0.90		0.91		0.96		0.99		0.97		0.90		0.94			8
7		---		0.95		0.91		0.92		0.95		0.98		0.97		0.93		0.73		---		7
6			---		0.94		0.91		0.94		0.98		0.98		0.95		0.78		---			6
5				0.99		0.92		0.94		0.97		0.99		0.96		0.90		0.72				5
4					0.96		0.94		0.97		0.99		0.98		0.89		0.92					4
3				---		0.96		0.96		0.99		0.99		0.93		0.90		---				3
2					---		0.99		0.98		0.99		0.96		0.82		---					2
1						---		1.02		1.01		1.00		0.95		---						1
0							---		1.04		1.03		1.01		---							0
-1								---		---		---		---								-1
-2											---											-2
	y	z	a	b	c	d	e	f	g	h	j	k	l	m	n	o	p	q	r	s	t	

Fast (>0.625 eV) Flux Ratios

34											---											34
33								---		---		---		---								33
32							---		0.62		0.67		0.63		---							32
31						---		0.66		0.86		0.86		0.66		---						31
30					---		0.84		0.93		0.96		0.93		0.49		---					30
29				---		0.77		0.93		1.05		1.02		0.91		0.50		---				29
28					0.63		0.99		1.02		1.05		1.04		0.71		0.85					28
27				0.64		0.89		1.00		1.04		1.08		1.04		0.65		0.62				27
26			---		0.91		1.00		1.08		0.94		1.09		0.90		0.79		---			26
25		---		0.95		0.99		1.03		0.99		0.96		1.12		0.86		0.92		---		25
24			0.95		1.04		1.05		1.01		1.00		1.09		0.93		1.05		0.97			24
23		---		1.07		1.12		1.02		1.09		1.01		0.98		0.99		1.08		---		23
22			1.08		1.10		0.85		1.03		1.01		1.08		0.93		1.11		1.12			22
21		0.69		1.01		1.02		0.95		1.02		1.12		1.02		1.10		1.15		0.78		21
20	---		0.92		1.00		0.96		1.02		1.06		1.10		1.10		1.16		1.08		---	20
19		0.71		0.99		0.97		1.00		1.02		1.03		1.10		1.14		1.08		0.99		19
18	---		1.02		0.99		0.97		0.97		1.00		1.07		1.12		1.04		1.10		---	18
17		0.66		1.06		0.99		0.99		1.01		1.05		1.02		1.20		1.10		1.13		17
16	---		0.95		1.11		0.97		1.03		0.99		0.99		1.12		1.12		1.13		---	16
15		0.72		1.05		1.02		1.00		0.96		0.98		1.02		1.12		1.23		1.12		15
14	---		1.04		0.96		0.95		0.94		0.96		1.01		1.12		1.13		1.11		---	14
13		0.65		0.98		0.99		1.00		0.96		0.98		1.05		1.15		1.08		1.12		13
12	---		0.89		0.99		0.87		0.95		1.08		1.09		1.05		1.09		1.12		---	12
11		0.72		0.96		1.03		0.87		0.98		0.99		0.92		1.10		1.07		1.07		11
10			1.01		1.01		0.81		0.98		0.99		1.01		0.85		1.01		1.17			10
9		---		0.99		0.97		0.92		1.06		1.02		1.05		0.80		1.04		---		9
8			1.03		0.98		0.79		0.93		1.02		1.05		0.96		0.97		1.10			8
7		---		1.13		0.99		0.84		1.06		1.06		1.05		0.99		0.98		---		7
6			---		1.15		0.92		0.95		1.08		1.04		1.05		1.02		---			6
5				0.85		1.19		1.02		0.98		0.97		0.98		1.19		0.83				5
4					0.88		1.11		1.03		0.93		1.00		0.97		1.02					4
3				---		0.77		1.21		1.05		1.05		0.99		0.98		---				3
2					---		0.90		1.22		1.13		1.21		0.96		---					2
1						---		0.92		1.21		1.21		1.15		---						1
0							---		0.90		0.93		0.95		---							0
-1								---		---		---		---								-1
-2											---											-2
	y	z	a	b	c	d	e	f	g	h	j	k	l	m	n	o	p	q	r	s	t	

--- incomparable site (full in TRIAD but partial in MCNP)

Figure 5 Flux map – MCNP ÷ TRIAD

Fission Power Ratios

34											...										34
33								...		...		...		...							33
32							...		...		...		...		...						32
31						...		...		...		...		...		...					31
30					...		...		...		...		...		...		...				30
29				...		...		...		1.03		1.00		...		...		...			29
28					...		1.02		1.02		...		1.01		...		...				28
27				...		...		1.01		...		...		...		...		...			27
26			...		...		0.99		...		...		1.01		...		...		...		26
25		...		...		0.99		0.99		1.01		...		1.03		...		...		...	25
24			...		1.01		...		1.00		1.01		...		...		1.05		...		24
23		...		1.02		...		0.95		...		0.98		...		...		1.08		...	23
22			...		...		...		0.99		1.00		1.03		...		1.09		...		22
21		...		...		1.00		...		0.99		...		...		1.08		1.11		...	21
20	...		...		...		...		...		1.00		1.02		1.07		...		...		...	20
19		...		0.98		0.99		0.95		0.94		...		...		1.08		...		...	19
18	...		...		0.97		0.95		...		...		0.98		1.05		...		1.13		...	18
17		...		...		0.95		0.89		0.95		0.98		...		...		1.10		...	17
16	...		...		...		...		...		...		...		1.04		1.10		1.12		...	16
15		...		1.00		...		0.92		0.92		...		0.98		1.06		...		...	15
14	...		...		...		...		...		0.96		0.98		...		...		1.12		...	14
13		...		...		0.95		0.88		0.93		0.97		0.98		1.04		1.10		...	13
12	...		...		0.97		...		0.88		...		...		...		...		1.09		...	12
11		...		0.95		0.95		...		0.93		1.01		...		...		1.03		...	11
10			...		...		...		0.89		0.97		1.02		...		...		...		10
9		...		0.95		...		0.89		...		1.02		1.02		...		0.94		...	9
8			...		0.95		...		...		1.01		1.02		...		...		...		8
7		...		...		0.93		...		1.00		1.04		1.01		0.93		...		...	7
6			...		...		...		...		...		...		0.98		...		...		6
5				...		...		0.97		...		...		...		...		...			5
4					...		...		0.99		...		1.00		...		...				4
3				...		...		...		0.99		0.99		0.93		...		...			3
2					...		...		...		...		...		...		...				2
1						...		...		...		...		...		...					1
0							...		...		...		...		...						0
-1								...		...		...		...							-1
-2											...										-2
	y	z	a	b	c	d	e	f	g	h	j	k	l	m	n	o	p	q	r	s	t	

... non-fuel site

Figure 6 Power map – MCNP ÷ TRIAD

MCNP can provide much more core data than TRIAD, such as the photon flux, the photoneutron source, or the heating rates (even in non-fuel materials, accounting for both neutron and photon sources). Also, MCNP could provide more correct *cdf*'s and extrapolation distances to be used in TRIAD to improve its results.

3.3 Outer NRU radiation

TRIAD is strictly limited to the inside of the reactor core (since the diffusion flux must vanish at the core extrapolated boundaries), but MCNP can transport particles anywhere in the model, making it possible to assess the radiation flux and dose rate in the outer structure of NRU, given the core as a radiation source of both neutrons and photons. MCNP is found to be very practical in this respect, since very accurate cores are not required.

Usually the criticality calculation (KCODE source option) is performed on an operating core at full power for radiation sources. By taking appropriate tallies, the radiation data (flux and dose rates) can be evaluated at locations of interest. Because of low fluxes in outer structures, many more source histories (resulting in longer computation time) and also additional techniques or analyses are required to obtain acceptable results. There is an obvious challenge to get satisfactory results at reasonable costs.

3.3.1 Ion chamber channels

There are three channels for collimating radiation beams towards the NRU ion chambers, starting from the re-entrant cans inside the reactor vessel and extending to the outer surface of the biological concrete shield (Figure 2). Figure 7 shows the MCNP flux and dose rate for both neutrons and photons in one such channel, filled with air in this analysis. The radiation flux and dose rate naturally decrease with distance away from the reactor core. With 500 million source histories, the data obtained are sufficiently accurate ($1\sigma < 5\%$) at the detector location, but become less reliable or even break down further out at the outer door where results are often needed. To add more, say 10 times, the number of histories (yielding 10 times longer computation time) would not help very much. In this case, since the neutron beam is well collimated in the hole leading to the ion chamber basket, it is appropriate to model a new mono-directional neutron source at this point and track the neutrons and secondary photons on down the channel. It is then found that the dose rate, either of neutrons or photons, at the channel door drops to roughly 10^{-4} of that in the detector space, with acceptable accuracy ($1\sigma \sim 6\%$; these results not shown in Figure 7).

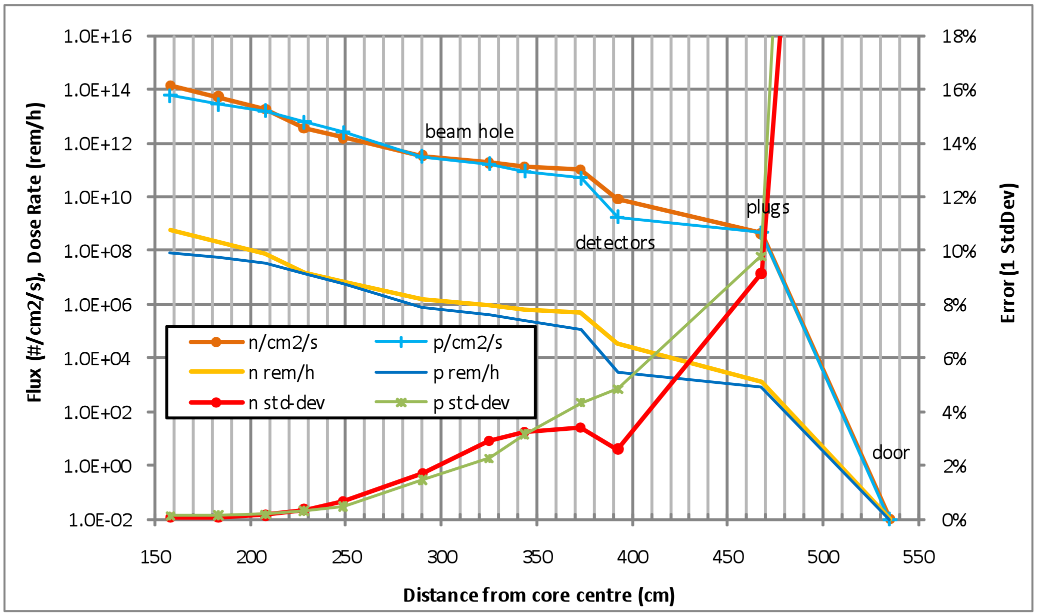

Figure 7 Radiation flux and dose rate along an ion chamber channel

Few photons from the reactor core reach the detector space (being gamma-shielded), and almost all photons present there are locally created from neutron interactions (i.e., these are neutron-induced photons). This is interesting because, during a reactor shutdown, the reactor photons (from fission product decay) should not pose a direct radiation hazard in the outer NRU structures; rather, the dose rate will come from a combination of reactor photoneutrons and the locally neutron-induced photons.

3.3.2 Thermal column

The fast (>1 MeV) neutron flux in the thermal column (Figure 2) was required for evaluation of the energy stored in NRU graphite. This Wigner energy accumulates due to fast neutrons displacing carbon atoms in the graphite lattice structure, and is subsequently released, at varying rates depending on the graphite temperature, giving rise to safety concerns.

Figure 8 illustrates the group flux variation moving from a reactor periphery site (NRU column A) to the outer of the first two graphite sections of the thermal column, HG1 and HG2. Although most neutrons leaving the reactor are of thermal energy (<0.625 eV), some fast neutrons manage to penetrate through HG1 and HG2. Like the thermal flux, the fast flux decreases moving away from the reactor but at a much greater rate (due to moderation in graphite and geometry). An MCNP calculation showed that the fast flux in the NRU thermal column is small enough, a maximum of 2.6E+09 $n.cm^{-2}.s^{-1}$ in HG1 and 1.1E+08 $n.cm^{-2}.s^{-1}$ in HG2, that it does not result in problematic amounts of stored energy in the graphite.

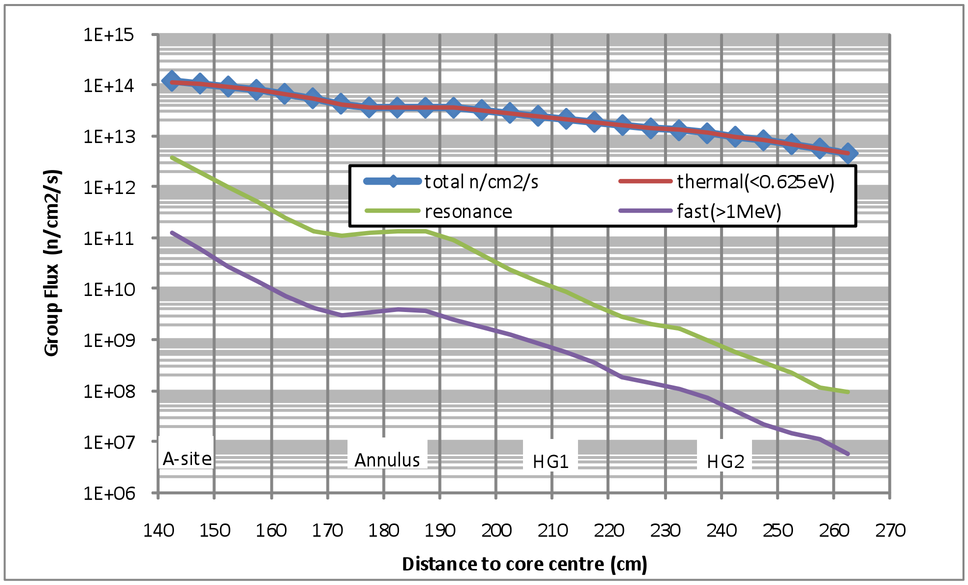

Figure 8 Neutron fluxes in thermal column sections HG1-HG2

Another practical application of MCNP is to assess the dose rate change when graphite is removed from a beam hole in the thermal column (for the purpose of work planning). Figure 9 presents the neutron flux and dose rate along the central beam hole of the thermal column, with graphite inserted or removed (replaced by air), through all five sections, HG1 to HG5, and then to the open door. Although the data at the door are not very accurate and should not be used directly, the points in the beam hole have logarithmic values well aligned to straight lines. Thus, the dose rate decreases exponentially with distance, dropping by a factor of 13 per meter of graphite and a factor of 5 per meter of air, respectively. As a result, the dose rate would increase ~2.6 times per meter of graphite removed from the beam hole.

It should be noted that the photon dose rate is only ~2-3% of the neutron dose rate, and usually is far less accurate. In fact, photons in remote outer locations of NRU are mostly induced by neutrons locally. Therefore, it is likely not worth trying to improve the photon data, but simpler to just add a few percent to the neutron dose rate to give a conservative total dose.

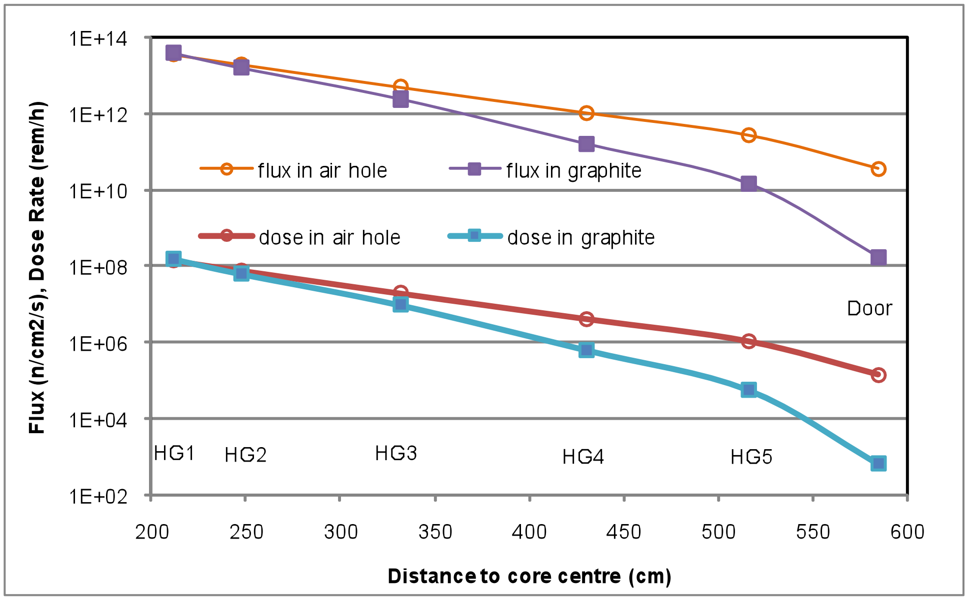

Figure 9 Neutron flux and dose rate in thermal column

4. Future challenges

4.1 TRIAD

The TRIAD code was initially written specifically to model NRU in hexagonal geometry, but with some modification it can handle reactor calculations with different lattice pitches and axial channel segmentation for the physics analysis of other reactor geometries. At present the maximum number of isotopes that the code can handle is limited to 150, and there is a need to modify the memory capacity to handle more isotopes, in order to cover a wider range of fuel types, if the code is used to analyze other reactors in the future.

Other upgrades to improve the performance of TRIAD are being considered, including:

- axial discontinuity factors,
- adjoint flux calculations,
- boundary condition respecification to improve leakage calculations,
- mesh refinement, and use of multi-cell WIMS model to improve flux calculations,
- extension to more than two energy groups,
- using a newer WIMS library with more groups and isotopes for cell parameters, and
- improving extrapolated distances and *cdf*'s using MCNP calculated results.

4.2 MCNP

There are three main challenges in advancing MCNP modelling of NRU: (i) improving radiation estimates at the outer surfaces of the reactor structures, (ii) increasing the possible number of burnup compositions, and (iii) implementing core following.

Future work to improve flux and dose rate calculations through the biological shield and the thermal column, without unacceptable increases in computer run time, will involve the use of various variance reduction techniques such as importance sampling and weight windows for the deep penetration problem, and DXTRAN spheres for the structure-hole streaming problem.

The limitation on the number of burnup compositions (and the number of isotopes in each composition) that can be handled is likely due to the addressable computer memory available on each node of our current cluster under the 32-bit WINDOWS operating system. The recently acquired 64-bit Linux-based cluster will likely mitigate this limitation. Testing is planned.

Finally, the prospect of using MCNP to replace TRIAD for day-to-day core following presents its own set of challenges. MCNP5 does not support burnup, thus, the code must be coupled with a depletion code, either externally as in Monteburns **[6]** or internally as in MCNPX **[7]**. These codes use MCNP to calculate isotope reaction rates, which are passed to the depletion code to advance burnup for a specified time step by calculating new isotope compositions for each burning material in the model. The neutron energy spectrum is also passed to the depletion code so that missing reaction rates can be supplied by the depletion code. The new material compositions are then returned to MCNP and the cycle repeats for the next time step. Monteburns supports multiple inner depletion time steps for each transport calculation, and the isotopes for which transport-calculated reaction rates are calculated is under user control. These features are not currently supported in MCNPX, thus, leading to much longer run times than with Monteburns.

Given the number of burning materials required for NRU core following (~80×14 for driver fuel plus isotope targets, loop fuel, and absorbers), the run times will likely be excessive for Monteburns and prohibitive for MCNPX. Nevertheless, feasibility will be investigated.

Another option that will be investigated is to use MCNP to determine only the fission power in each burning material and then use a coupling code to advance the burnup by interpolating in a set of WIMS pre-calculated compositions tabulated as functions of fuel type and burnup. While this method does not have transport-depletion two-way coupling (the WIMS burnup is still done in fixed environments like WIMS/TRIAD), it does offer the potential of better power distributions than TRIAD and faster run times than either Monteburns or MCNPX. Such a WIMS/MCNP coupling code has already been developed but has seen limited testing or use.

A final consideration in the decision to adopt MCNP for NRU core following is that a sophisticated user interface has been developed for TRIAD that simplifies fuel and isotope rod movements, and automatically tracks rod identifiers, compositions, and burnups. Such an interface does not exist for MCNP; the development of this capability would require considerable effort.

5. Summary

The TRIAD code has been successfully applied to the day-to-day operation of the NRU reactor for 20 years. However, there is room for improvement to extend its capability to include axial discontinuity factors, mesh refinements, more energy groups, and more isotopes to cover a wider range of fuel types. With further modifications to the lattice pitches and axial channel heights, it could handle physics analyses of other types of reactors.

A full-reactor MCNP model of NRU has been developed for benchmarking the TRIAD core results. While the key parameters from the two methods are in reasonably good agreement, the MCNP method appears to eliminate the known *k*-eff bias in TRIAD. Moreover, MCNP is able to provide other kinds of data beyond the reach of TRIAD, such as photon transport and energy deposition data, as well as radiation flux and dose rate outside the reactor core. Besides being very computer run-time intensive, the MCNP method currently has a limited total number of burnup compositions and/or fission product nuclides used in the model, making it unsuitable for practical applications.

Investigation into the use of variance reduction to improve the calculation of neutron and photon fluxes and dose rates outside the reactor core, and the use of computers with more addressable memory to improve burnup capability, will be pursued since these initiatives have the potential to yield tangible improvements to NRU modeling with MCNP that will be of immediate benefit. The value of developing MCNP-based core following is less obvious. At present it is unclear whether the potential improved accuracy over TRIAD is warranted given the development costs and the substantial increase in computer resources required, particularly for a reactor that could see little more than five years of remaining service.

6. Acknowledgment

The authors would like to thank M. Atfield for his contribution.

7. References

[1] S.R. Douglas, "A calculational model for the NRU reactor", Paper presented at the Canadian Nuclear Society 1985 Annual Conference, also AECL Report AECL-8841, 1985 June.

[2] J.D. Irish and S.R. Douglas, "Validation of WIMS-IST", Proceedings of the 23rd Annual Conference of the Canadian Nuclear Society, Toronto, Ontario, Canada, 2002 June 2-5.

[3] T.C. Leung and M.D. Atfield, "Validation of the TRIAD3 code used for the neutronic simulation of the NRU reactor", Proceedings of the 30th Annual Conference of the Canadian Nuclear Society, Calgary, Alberta, Canada, 2009 May 31 - June 3.

[4] X-5 Monte Carlo Team, "MCNP – A general Monte Carlo N-particle transport code, version 5", Los Alamos National Laboratories, LA-UR-03-1987 (revised 2005).

[5] T.S. Nguyen and R.E. Donders, "Study of end peaking power for NRU loop fuel calculations", Proceedings of the 31st Annual Conference of the Canadian Nuclear Society, Montreal, Quebec, Canada, 2010 May 24-27.

[6] D.L. Poston, and H. R. Trellue, "User's manual, version 2.0 for MONTEBURNS version 1.0," Los Alamos National Laboratory report, LA-UR-99-4999, 1999 September.

[7] D.B. Pelowitz, ed., "MCNPX user's manual, version 2.7.0," Los Alamos National Laboratory report, LA-CP-11-00438, 2011 April.